

# A NEW PRODUCTID BRACHIOPOD FROM THE UPPER VISÉAN OF SCOTLAND

by K. A. G. SHIELLS

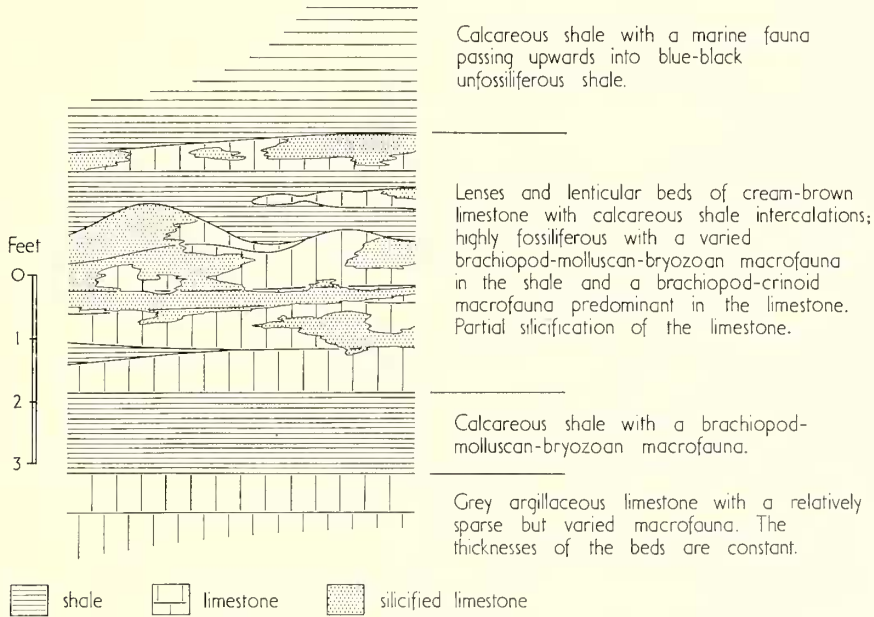
ABSTRACT. *Promarginifera trearnensis* gen. et sp. nov. a productid brachiopod from the Upper Viséan of Ayrshire, Scotland is described. It occurs in the Dockra Limestone 65 ft. below the Viséan–Namurian junction. Morphologically the form has affinities with both the marginiferids and dictyoclostids but on the evidence of a marginiferid cardinal process and discontinuous marginal ridges it is classified as a marginiferid of the subfamily Costispiniferinae.

SPECIMENS of an unrecorded productid have been collected from the Upper Viséan of Ayrshire, Scotland. The form was first found at Trearne quarry (NS 37155340) 1.4 miles N. 108° E. of Beith, and has subsequently been obtained from the neighbouring Hessilhead quarry (NS 37755315) 0.4 miles N. 288° E. of Hessilhead Farm. Both of these quarries expose the Dockra Limestone, here 20–25 ft. thick, and up to 10 ft. of the overlying argillaceous succession. The base of the Dockra Limestone locally occurs 10 ft. above the base of the Lower Limestone Group of Scotland and is approximately 65 ft. below the shale underlying the Top Hosie Limestone which is considered on the evidence of *Cravenoceras scoticum* within the limestone and *Cravenoceras* sp. indet., within the shale to approximate to the Viséan–Namurian boundary (Currie 1954, pp. 534, 535). The Lower Limestone Group which is 80 ft. thick in the Beith district consists of a 95% calcareous-argillaceous succession; the massive section of the Dockra Limestone thins from 35 ft. near Dalry to 13 ft. near Lugton, being replaced in a west to east direction by shales and alternations of shales and limestone bands (Richey, Anderson, and MacGregor 1930, pp. 141–8, fig. 12).

The Dockra Limestone is in part lenticular with the development of a shell-bank facies of cream-coloured limestones within dark, thinly bedded, argillaceous limestones. Text-fig. 1 illustrates a measured section on the east end of the working north face of Trearne quarry which was accessible in May 1964. Cream-brown lenticular bedded calcarenites overlie a shale parting which in turn rests on grey argillaceous calcilutite forming the uniformly bedded upper portion of the main calcareous unit. The lenses of calcarenite are highly fossiliferous, the organic content of some is 90% composed of productids and crinoid remains, the brachiopod valves forming a shell-supported fabric with the interstices infilled with crinoid debris and matrix. These shell-bank accumulations were deposited in a moderately turbulent environment. The productids in the lenses include species of the genera *Productus*, *Krotovia*, *Buxtonia*, *Antiquatonia*, *Eomarginifera*, and *Promarginifera* gen. nov.; in some of the lenses *Promarginifera* forms 95% of the productid fauna.

The material for this study was collected from Trearne quarry. The specimens are preserved in three different ways: (i) calcareous shells in a calcareous matrix—the normal unreplaced condition, (ii) siliceous shells in a siliceous matrix—complete silicification of the rock either along layers parallel to the bedding or in irregularly shaped masses of

scattered distribution, (iii) siliceous shells in a decomposed ochreous matrix—the most useful, but relatively rare material. The visceral cavities of all the partially or completely silicified shells and 90% of the calcareous shells are infilled with a drusy growth of transparent quartz. Incomplete silicification and the growth of the quartz crystals within the visceral cavity have been responsible for the imperfection of internal detail observed in most specimens. Furthermore the infilling is stronger than the shell substance



TEXT-FIG. 1. Vertical section through the upper beds of the Dockra Limestone at Trearne Quarry, Ayrshire.

and its removal from the visceral cavity difficult. It is evident from the nature of the deposition of the *Promarginifera*-bearing lenses that the brachiopods are not found in their growth positions but have undergone varying degrees of reworking. This movement damaged the shells, especially stripping them of their spines and breaking the ears and trail. In a collection of approximately 500 specimens only 119 were sufficiently well preserved for statistical analysis. Of the latter, 62 specimens show the exterior surface of the pedicle valve, 7 of these also show the pedicle valve interior, and 37 others also show the brachial valve exterior. The remaining 57 specimens are fragmental brachial valves showing both interior and exterior surfaces. The collection on which the statistical analysis is based is deposited in the Hunterian Museum in the University of Glasgow. All linear measurements are given in millimetres, angular measurements in degrees.

## SYSTEMATIC DESCRIPTION

Suborder PRODUCTOIDEA Maillieux 1940

Superfamily PRODUCTACEA Waagen 1883

Family MARGINIFERIDAE Stehli 1954

Subfamily COSTISPINIFERINAE Muir-Wood and Cooper 1960

Genus PROMARGINIFERA gen. nov.

Plate 67, figs. 1-14

*Derivation of name.* Latin, *pro*—early; *marginifera*—margin bearer.

*Type species.* *Promarginifera trearnensis* sp. nov.

*Diagnosis.* Shell subquadrate, costate and rugate, with reticulate umbo. Spinose pedicle valve, spines arranged (i) in row along ear, (ii) in row down flank, (iii) scattered over valve on costae. Ears large and enrolled, demarcated from flank by sharp fold. No geniculation or thickening of trail of brachial valve. Non-crenulate marginal ridges extending laterally from cardinal process parallel to hinge-line. Dendritic, elevated adductor scars, variable cardinal process. Pedicle valve with flabellate diductor scars and adductor platform.

*Description.* Shell small, subquadrate, width exceeds straight length. Pedicle valve convex, flanks approximately normal to hinge-line at the posterior before curving anteriorly on to a broad venter; venter with or without sulcus, trail curved; flanks moderately steep and umbo incurved forming a uniformly convex visceral disc; ears large and enrolled, demarcated from flanks by sharp fold. Brachial valve with posterior of visceral disc plane or slightly concave, becoming rounded and concave anteriorly to form trail, no geniculation; trail is a single structure and is not thickened by additional laminae.

Both valves costate and rugate, umbonal region reticulate. Pedicle valve with erect or suberect spines, arranged, (i) in row near hinge margin, (ii) in curved row down flanks, and (iii) scattered over the visceral disc, venter, and flanks on supracostal positions. A few scattered spines may be present on the brachial valve.

Interior of pedicle valve with flabellate diductor scars which are longitudinally ridged and separated from each other by an elevated platform bearing two ovate adductor scars; the ears are demarcated from the visceral cavity by a sharp flexure.

Interior of the brachial valve with trilobate marginiferid cardinal process which may be highly variable in its attitude with respect to the posterior part of the valve and in the degree of separation of the lateral lobes; posteriorly the median septum is low and rounded or ill defined, anteriorly it extends into a blade-like structure; away from the median septum the marginal ridges follow close to the hinge-line and then swing anteriorly along the inner margin of the ears to finally die out on the flanks; brachial ridges are narrow, low, sometimes obscure, given off at anterior-lateral margin of adductor scars at a low angle to the hinge-line direction; each adductor has a double dendritic surface within the attachment area, the anterior scar being upraised along its anterior border; rows or scattered endospines occur anteriorly.

*Remarks.* *Promarginifera* combines both dictyoclostid and marginiferid characters. The reticulate umbo, flabellate diductor scars, adductor platform, and dendritic adductor

scars are features usually associated with dictyoclostids. On the other hand the cardinal process is of a type strictly comparable to that found in the marginiferids and the possession of the marginal ridges is an essential character of that group. Furthermore, both the size and shape of the shell and the large, enrolled, well-demarcated ears are like those found in many marginiferids. The striking arrangement of spines on the pedicle valve of *Promarginifera* is not completely diagnostic since it is similar to that of several other genera including dictyoclostids such as *Antiquatonia* and *Costiferina*, marginiferids such as *Costispinifera* and *Liostella*, and the alleged buxtoniid *Protoniella*. An assessment of the taxonomic placing of *Promarginifera* suggests, therefore, that it is a marginiferid with dictyoclostid similarities. Since the marginiferids almost certainly evolved from the dictyoclostids in Lower Carboniferous times the balance or morphological attributes found in *Promarginifera* (a high Lower Carboniferous form) may indicate phylogenetic affinity with a dictyoclostid stock.

According to Muir-Wood and Cooper (1960, p. 205) two of the four subfamilies of the Marginiferidae, the Marginiferinae and the Costispiniferinae, are separated on internal features, especially in the degree of completeness of the marginal ridges. The condition in which the marginal ridges fuse anteriorly to form a continuous rim around the anterior of the visceral disc characterizes the Marginiferinae. If the marginal ridges are discontinuous and die out anteriomedianly the form belongs to the Costispiniferinae. The remaining two subfamilies of the Marginiferidae have special features such as the tubiform trail and row of endospines in the brachial valve of the Retariinae and the supplemented brachial trail of the Probolioniinae.

*Promarginifera* has certain external resemblances to the genera *Marginifera* and *Hystericulina*, both members of the subfamily Marginiferinae. The general shape and size of the shells, the dimensions of the costae, and to a lesser extent, the distribution of spines, are similar in all three genera. Another marginiferinid, *Eomarginifera*, is found associated with *Promarginifera* but can be easily distinguished externally by its six symmetrical spine bases. In internal detail, however, *Promarginifera* has discontinuous marginal ridges and is therefore distinct from the marginiferinids; it is clearly a member of the Costispiniferinae and is the first British genus to be ascribed to that group. *Promarginifera* shares some external features with other members of the Costispiniferinae, notably with *Costispinifera*, *Liostella*, and *Elliotella*. *Promarginifera* can be distinguished from *Costispinifera* by its less numerous spines, non-crenulate marginal ridges, non-geniculate but more costate brachial valve, and shorter endospines. Externally the pedicle valve of *Promarginifera* differs from that of *Liostella* in having a reticulate umbo and a row of spines on the ears close to the hinge-line. Internal distinctions include the more elevated and smooth marginal ridges of *Promarginifera* and differences in detail of the cardinal process, median septum, and adductor scars. *Elliotella* is more coarsely costate than *Promarginifera* and does not possess rugae on the pedicle valve. The orientation of the two spine rows near the hinge of *Elliotella* is different from that of *Promarginifera*. Internally, the marginal ridges of both *Elliotella* and *Costispinifera* diverge from the hinge immediately after leaving the cardinal process; they cannot, therefore, buttress the articulating surface as do those of *Promarginifera* (see description of *P. trearnensis*). The genus *Protoniella* simulates *Promarginifera* externally, particularly in the distribution of the spine bases; internally, however, they can be readily distinguished by the buxtoniid cardinal process and antron of the former.

*Promarginifera trearnensis* sp. nov.

Plate 67, figs. 1-14

*Diagnosis.* As for genus.*Type specimens.* The type series consists of a holotype and 118 paratypes, the total collection on which the statistical analysis is based.

Specifications of the holotype: Hunterian Museum number L6202; Plate 67, figures 1, 2, 3:

Hinge width	19.5 mm.
Curved length of pedicle valve	29.0 mm.
Straight length	13.4 mm.
Thickness of visceral cavity (inclusive of shell)	6.0 mm.
Umbonal angle	90°
Extension of umbo posterior to hinge-line	0.7 mm.
Width of ears	8.5 mm.
Length of ears	3.6 mm.
Height of ears	0.7 mm.
Number of rugae	4
Number of costae	24
Nonsulcate; width of flat zone on venter	2.0 mm.
Number of spines on pedicle valve exterior	99

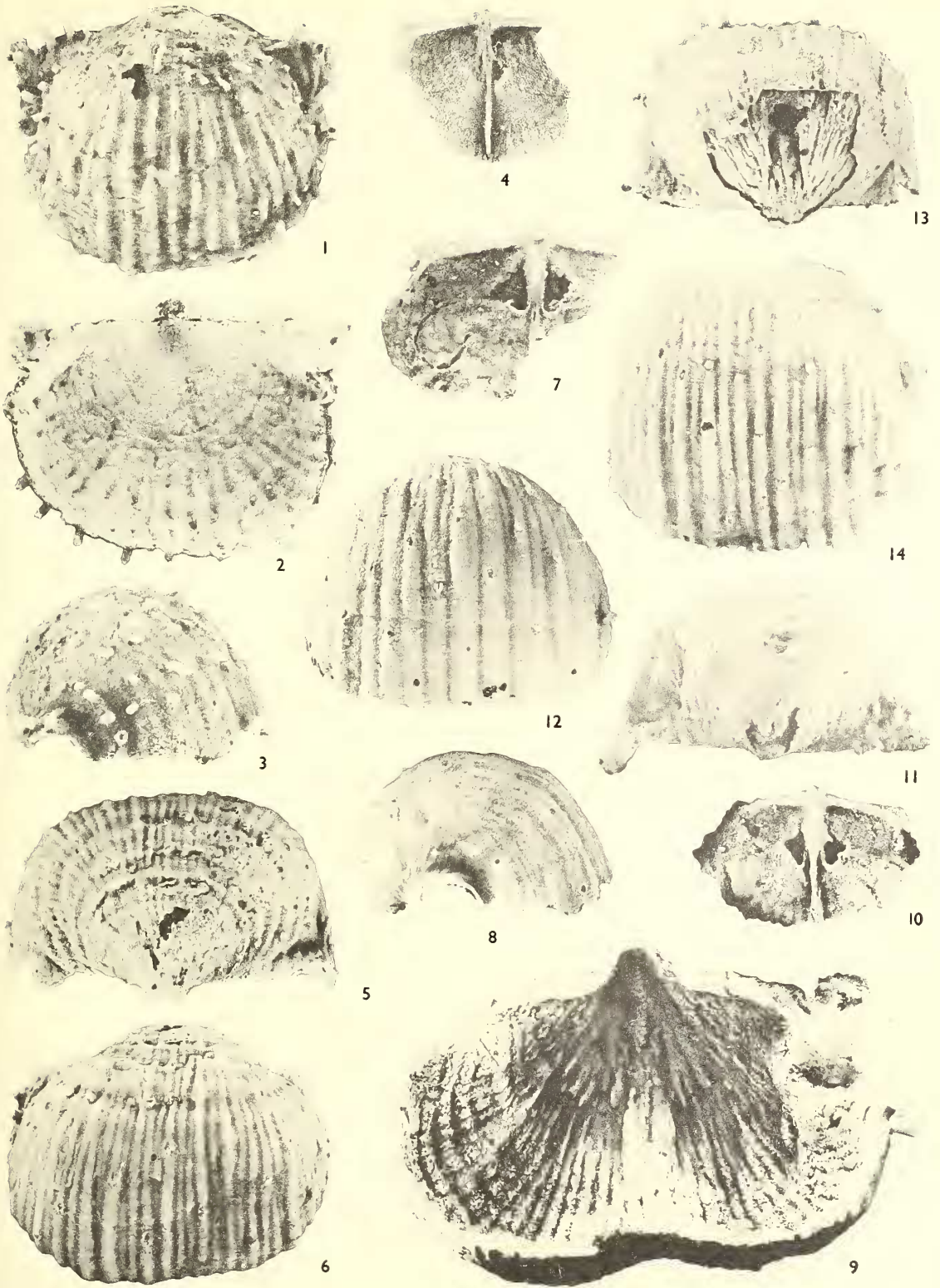
The figured paratypes (Pl. 67, figs. 4-14) are given Hunterian Museum numbers L6203-11, and the remaining paratypes are given Hunterian Museum numbers L6212/1-107.

*Description.* The shells are small (Muir-Wood and Cooper 1960, p. 18) with a sample mean hinge width (= maximum width) of  $17.3 \pm 1.0$  mm. The size of the species is more fully described by the statistics of Table 1 (all confidence limits are quoted at the 0.01 level of probability unless otherwise stated). The shell outline is subquadrate (Pl. 67, figs. 1, 3, 5); the outer surface of the pedicle valve is strongly convex and the outer surface of the brachial valve is strongly concave; neither valve is geniculated (text-fig. 2). The curvature of the posterior to anterior profile of the pedicle valve in the median plane of the shell (text-fig. 3, method after Prentice 1956) is a compound of three logarithmic spirals which from umbo to trail have spiral angles of 37°, 44°, and 81° respectively, the initial spiral being subject to secondary modification and is not precisely defined. In all

## EXPLANATION OF PLATE 67

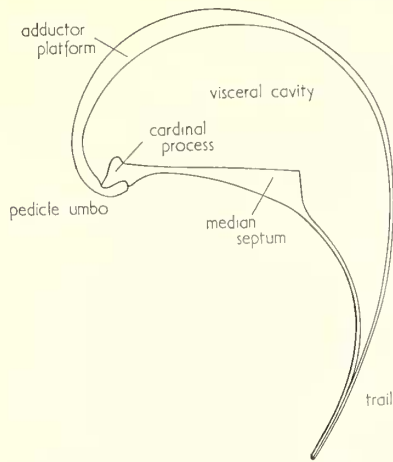
*Promarginifera trearnensis* gen. et sp. nov.

- Figs. 1-3. Holotype; Hunterian Museum L6202. 1, ventral view; 2, dorsal view; 3, lateral view.  $\times 3$ .  
 Fig. 4. Paratype; H.M. L6209. Interior of brachial valve showing cardinal process of type 1.  $\times 2.5$ .  
 Figs. 5-6. Paratype; H.M. L6204. 5, posterior view showing reticulate umbo; 6, ventral view showing costation of type 2.  $\times 3$ .  
 Fig. 7. Paratype; H.M. L6211. Interior of brachial valve showing cardinal process of type 5.  $\times 2.5$ .  
 Fig. 8. Paratype; H.M. L6207. Lateral view showing enrolment of ear.  $\times 3$ .  
 Fig. 9. Paratype; H.M. L6208. Interior of pedicle valve showing diductor scars and adductor platform.  $\times 4$ .  
 Fig. 10. Paratype; H.M. L6210. Interior of brachial valve showing cardinal process of type 6.  $\times 2.5$ .  
 Fig. 11. Paratype; H.M. L6203. Posterior view.  $\times 2.5$ .  
 Fig. 12. Paratype; H.M. L6206. Antero-ventral view showing costation of type 6.  $\times 3$ .  
 Figs. 13-14. Paratype; H.M. L6205. 7, posterior view showing internal mould of diductor scars and adductor platform; 8, antero-ventral view showing costation of type 3.  $\times 2.5$ .

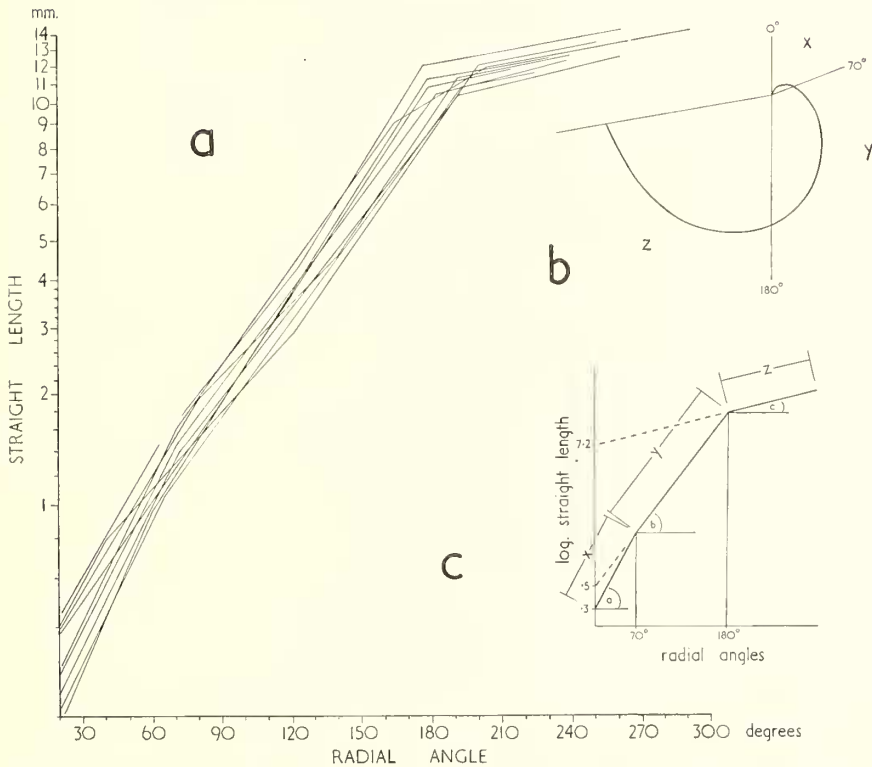


SHIELLS, Carboniferous *Promarginifera* gen. nov.





TEXT-FIG. 2. A median section of the shell of *P. trearnensis* showing the profile of the valves, the thickening of the pedicle valve in the region of the adductor platform, and a large cardinal process.

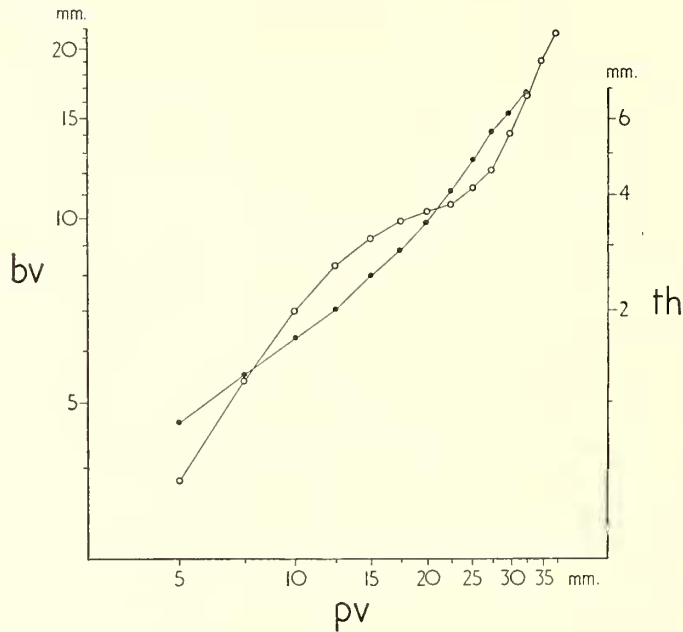


TEXT-FIG. 3. A plot of the straight length vectors which describe the growth spirals of the curved length of the pedicle valve. The principal changes in slope of the nine profiles plotted on (a) represent the change in spiral of the curves x, y, and z on (b). This is shown on the summation diagram (c) and the angles a, b, and c are the spiral angles.

specimens the hinge-line is straight and the hinge width is the maximum width of the shell; neither valve possesses an interarea.

#### GROWTH OF VALVES

The relative growth of the two valves and the increase in the thickness of the visceral cavity of *P. trearnensis* follow a pattern for strongly concavo-convex productids which is discussed elsewhere (Shiells 1965, pp. 878–80). Since the curvature of the valves is constant (within 5% angular variation), measurements of any individual of the sample population broadly characterize the species as a whole.



TEXT-FIG. 4. A plot on logarithmic coordinates of uniform growth increments to the curved length of the pedicle valve (*pv*) against (i) the corresponding increments to the curved length of the brachial valve (*bv*) shown as dots, and (ii) the corresponding increments to the thickness of the visceral cavity (*th*) shown as open circles.

It is observed that:

1. For unit increase in the growth of the curved length of the pedicle valve, the corresponding consecutive growth increments to the curved length of the brachial valve (*a*) systematically diminish until the pedicle valve has reached a length of approximately 22.5 mm., (*b*) progressively increase as the pedicle valve grows from approximately 22.5 to 32.5 mm., and (*c*) are equal in length for the remainder of growth (Table 2, text-fig. 4). From the first reliable measurements, i.e., when the curved length of the pedicle valve equals 5 mm., and the curved length of the brachial valve equals 3.8 mm., to the growth stage in which the curved length of the pedicle valve equals 11 mm., and the curved length of the brachial valve equals 7.5 mm., there is a simple allometric growth relationship between the valves. The allometric growth constant is 0.87 (text-fig. 5*a*). Subsequent growth of the two valves, however, deviates from simple allometry. As the two valves increase in curved length to approximately 22 mm. and 10.5 mm. for the pedicle and brachial respectively, there is a systematic decrease in the value of the allometric coefficient from 0.87 to 0.2. From this point until the growth stage in which

the curved length of the pedicle valve is 32.5 mm. and the curved length of the brachial valve is 16.5 mm., the values of the allometric coefficient rapidly increase to 1.98. Due to the parallelism of the valves further values for the allometric coefficient decrease until growth ceases.

2. For unit increase of the curved length of the pedicle valve as above, the corresponding increments to the thickness of the visceral cavity (*a*) are constant at first and then progressively increase until the pedicle valve has attained a length of approximately 27.5 mm., and (*b*) successively decrease as the pedicle valve increases from approximately 27.5 mm. to 32.5 mm. (Table 2, text-fig. 4). When the growth of the pedicle valve reaches approximately 32.5 mm., the brachial valve has become parallel to the pedicle valve. Since no specimen of *P. trearrrensis* shows any thickening of the existing brachial valve or secretion of a new trail to the brachial valve, it follows that no further increase in the thickness of the visceral cavity can take place once this condition has been achieved. Allowing for a total maximum variation in the thickness of the shell substance of the valves, the sulcation, and costation, the estimate of the maximum thickness of the visceral cavity inclusive of the shell is  $8 \pm 1.5$  mm. As shown on text-figure 5*b* an isometric growth relationship (coefficient of allometry equal to unity) exists between the thickness of the visceral cavity and the curved length of the pedicle valve, until the latter reaches 17.5 mm. For further increase in the curved length of the pedicle valve, subsequent coefficients of allometry successively rise to a maximum value of 1.7, corresponding to a curved length of the pedicle valve of 27.5 mm. Finally, the values of the coefficient of allometry diminish in turn to 0.95 when the maximum thickness of the visceral cavity is attained.
3. For unit increase in the growth of the curved length of the brachial valve, the corresponding consecutive growth increments to the thickness of the visceral cavity (*a*) maintain a fairly constant size at first until the curved length of the brachial valve is 9.9.5 mm., (*b*) progressively increase as the curved length of the brachial valve is extended to 13–13.5 mm., and (*c*) successively diminish until the parallelism of the valves prevents further enlargement of the visceral cavity (Table 3, text-fig. 6). The relative growth of the thickness of the visceral cavity and the curved length of the brachial valve is shown on text-fig. 5*c*; the deviations from standard allometry are complex.
4. As shown on Table 4 the correlation of the hinge width with the curved length of the pedicle valve and the straight length is significant at a high level. However, such a correlation is subject to two interpretations. Firstly, in the light of the complex growth relationships between the curved lengths of the two valves it might be expected that an equally involved relationship would exist between the length of a valve and the hinge width, the correlation of the total data simply averaging the effect of the sample distribution about the true growth curve of the two characters. The growth of the two valves is controlled, however, by the common origin and common line of termination of any growth stage. In a comparison of the length with the width of the shell there is no similar direct functional dependence although an indirect cause is presumed. In the second place, therefore, it is possible that the growth of the hinge width matched that of either of the valves largely to substantiate the correlation. Unfortunately the growth laminae on the external surface of the shell proved insufficiently distinct to test these possibilities.

The slope of the flanks is inclined 65–80° depending on the completeness of the trail (Pl. 67, figs. 6, 11, 14). The shape of the venter is slightly convex, approximately flat, or sulcate (Table 1, Pl. 67, figs. 1, 5, 9, 12, 13). Of 44 specimens 18 (41%) possessed a sulcus and 26 (59%) were nonsulcate. A gradation exists between (i) nonsulcate forms, (ii) forms with a closed sulcate depression restricted to the anterior part of the visceral disc and the posterior end of the trail, and (iii) forms with an open sulcus beginning on the anterior part of the visceral disc and extending to the anterior extremity of the trail. The sulci of the open type are deepest on the anterior part of the visceral disc and the posterior end of the trail as demonstrated by the data of Table 5. Examination of the degree of correlation between the maximum width and maximum depth of the sulcus on 18 specimens just failed (by 0.001) to be significant at the 0.05 level of probability (Table 4). No significant correlation occurs between the height of the visceral cavity and the inward folding of the venter as possibly anticipated if the sulcation represented a simple structural modification of the test to strengthen an increasingly arched internal lumen (Table 4).

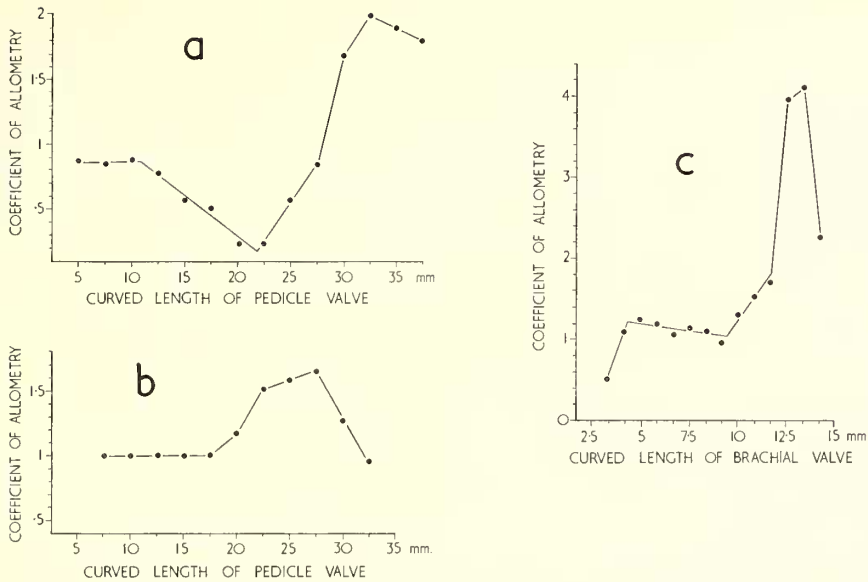
The umbo shows moderate expansion with a mean umbonal angle of  $99.5 \pm 4.8^\circ$  (Table 1). In all specimens the umbo projects posterior to the hinge (Table 1, Pl. 67, figs. 3, 6, 11, 14). Inflation of the umbonal cavity is expressed by corresponding increments (correlated at the 0.05 level of probability) to the umbonal angle and the distance to which the umbo extends posterior to the hinge (Table 4). Such inflation accompanies a general increase in gibbosity of the visceral cavity as shown by the significant correlation at the 0.05 level of probability between the height of the visceral cavity (plus the shell thickness of each valve) and the extension of the umbo posterior to the hinge. However, the very low (not significant) correlation between the hinge width and umbonal angle (indeed a low negative value was obtained—Table 4) suggests that an overall volumetric increase in the capacity of the shell interspace is not necessarily a function of gibbosity.

Prominent ears are an intrinsic feature of *P. trearnensis* (Pl. 67, figs. 1, 3, 8, 9). In shape they are triangular and enrolled, approximating either to a cylindrical sector or to a conical sector increasing in width and curvature towards the postero-lateral extremities. The mean dimensions of the structures are given on Table 1. Although the correlation between the width of the ear and the hinge width is significant at the 0.01 level and the correlation between the ear width and ear length is significant at the 0.05 level, the height of the ear, a measure of its curvature or degree of enrolment, varies independently (Table 4). The steeply inclined enrolled anterior slopes of the ears oppose the steeply inclined umbonal lateral surfaces to form a conspicuous groove, which either demarcates the slant side of the conical sectors or traces obliquely round the more cylindrical types of ear surface, increasing in depth towards the lateral margin of the shell.

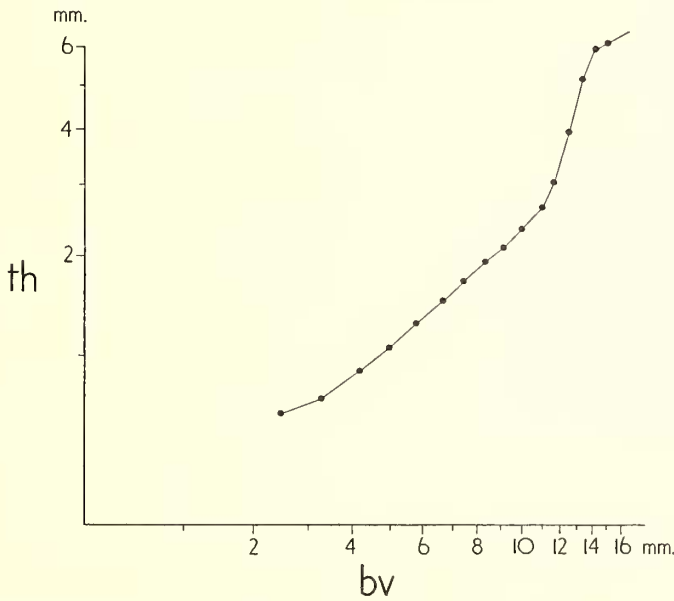
#### EXTERIOR OF PEDICLE VALVE

The exterior surface of the pedicle valve is conspicuously costate (Pl. 67, figs. 1, 5, 12, 13), the mean number of costae being  $26 \pm 2$  at the anterior margin (Table 1). Alternate costae and sulci diverge from an umbonal focus, each costa and sulcus proportionately increasing in width towards the anterior. The spread of the fan of costae is supplemented on the central, anterior, and antero-lateral regions of the visceral disc through additional costae being inserted or produced by bifurcation. On reaching the anterior of the visceral disc or the posterior part of the trail, expansion ceases and the costae and intercostal sulci continue as a set of parallel ridges and grooves down the length of the venter and antero-lateral surfaces of the trail to the valve extremity. Rarely, coalescence of costae takes place on the trail. Three properties of the costation (text-fig. 7), (i) the maximum widths of the costae attained on any specimen, (ii) the regularity of costation, and (iii) the shape or combinations of shape of the costae in transverse section, have been used to arbitrarily subdivide the continuously variable pattern for descriptive purposes. The six groups into which the costation may be subdivided are given in Table 6. The costation of 50 specimens has the following distribution; group 1—10 specimens (20%), group 2—9 specimens (18%), group 3—16 specimens (32%), group 4—8 specimens (16%), group 5—6 specimens (12%), and group 6—1 specimen (2%).

The exterior surface of the pedicle valve is rugate (Pl. 67, figs. 6, 11); the mean number of rugae is  $7 \pm 1$  (Table 1). The trace of the rugae and interrugal sulci approximates to a series of semi-ellipses about an umbonal origin. The majority of the rugae traverse the visceral disc but 0–2 of the inner rugae and 1–3 of the outermost rugae die out on the

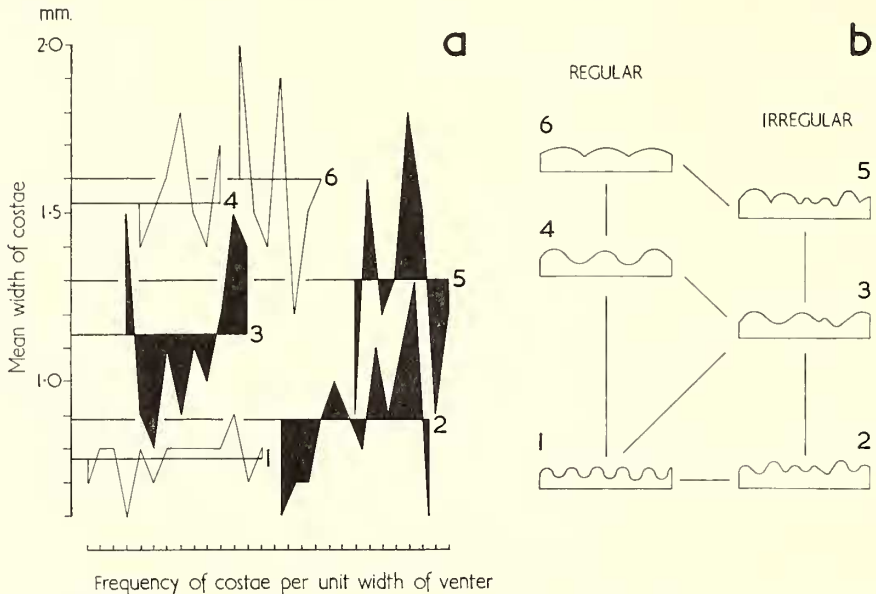


TEXT-FIG. 5. Deviations from simple allometry: (a) Coefficient of allometry for the relative growth of the length of the brachial valve and the length of the pedicle valve plotted against the length of the pedicle valve, (b) Coefficient of allometry for the relative growth of the thickness of the visceral cavity and the length of the pedicle valve plotted against the length of pedicle valve, and (c) Coefficient of allometry for the relative growth of the length of the brachial valve and the thickness of the visceral cavity plotted against the length of the brachial valve.



TEXT-FIG. 6. A plot on logarithmic coordinates of uniform growth increments to the curved length of the brachial valve (*bv*) against the corresponding increments to the thickness of the visceral cavity (*th*).

umbonal slopes. As the distance from the umbo increases there is a proportionate increase in the dimensions of the rugae. Furthermore, each of the outer rugae changes shape from an approximately equidimensional structure at the base of the umbonal slopes to one in which the posterior to anterior width of the ruga exceeds the height by a maximum factor of ten. Eight per cent. of the rugae bifurcate across the visceral disc. Measurements from a single specimen to demonstrate the progressive change in size of the rugae are given on Table 7. The rugae and costae lie normal to one another over the

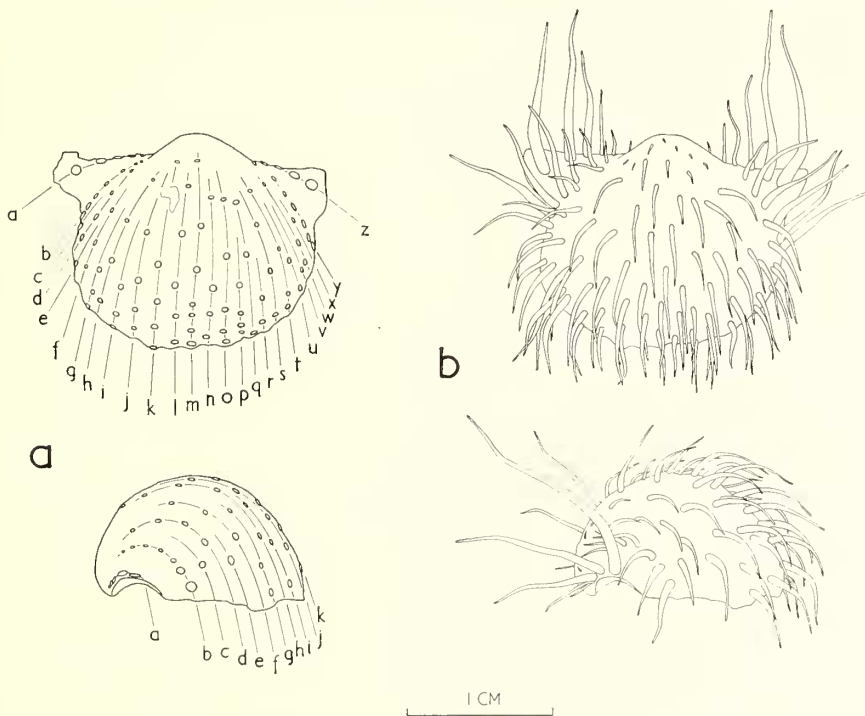


TEXT-FIG. 7. Variation of costation on the pedicle valve. The costation is arbitrarily grouped into six categories on the basis of regularity, size, and shape (*b*). Plots of examples of these groupings are shown on (*a*).

shell surface of the posterior region of the visceral disc, and the incidence of costae, intercostal sulci, rugae, and interrugal sulci produces a reticulated pattern. Close to the umbo the internodal intercepts on a costa are approximately twice the internodal intercepts on a ruga. However, as the rate of expansion of the rugation pattern exceeds that of the costation, the reticulation becomes progressively elongate in an anterior direction so that the internodal intercepts on a costa approaching the central part of the visceral disc are four times the internodal intercepts on a ruga in the same region. Measurements from a single specimen to show this relationship are given in Table 8. No significant association occurs between the type of costation and the number of rugae ( $\chi^2$  contingency only shows correlation at the 0.95 level of probability). The limitation of the rugae to the posterior surface of the visceral disc suggests that such corrugation may structurally reinforce the tightly convex umbonal slopes; however, no significant correlation ( $r = -0.244$ ) occurs between the frequency of the rugae and the size of the visceral cavity.

The pedicle valve is highly spinose with 50–100 erect, or suberect, halteroid spines projecting from its surface (text-fig. 8; Pl. 67, figs. 1, 2, 11, 13). The spines are situated on

radii of umbonal origin and the spine bases progressively increase in diameter away from the umbo. The two spine rows on each side of the umbo which are closest to the hinge-line are especially distinct. They are characterized by a more regular spacing of the spine bases and, for an equivalent distance from the umbo, the spine bases are slightly greater in diameter than those on the remainder of the valve (Table 9). The posterior row is situated on the posterior enrolled slope of the ear and is subparallel to the hinge-line (maximum divergence from the hinge-line  $15^\circ$ ). The anterior row is situated down the



TEXT-FIG. 8. Spinosity of the pedicle valve (ventral and lateral views). (a) Plot of spine bases on the holotype showing their distribution on 26 radii of umbonal origin (*a-z*); spine rows *b* to *y* are supracostal; spine rows *a* and *z* occur on the ventral and posterior ear slopes. (b) Reconstruction of spines; positions of the spine bases as for holotype, length and curvature of spines based on collective information.

flank and initially diverges from the posterior row at an angle of  $25-30^\circ$ . All of the spines are supracostal except those on the ears and those on the posterior part of the row down the flanks.

The exterior surface of the pedicle valve shows concentric growth lamellae; the frequency of the lamellae is of the order of 7-9 per mm.

#### INTERIOR OF PEDICLE VALVE

The interior of the pedicle valve is strongly concave and is for the greater part an exact reflection of the convex exterior. The internal ridges and furrows which radiate from the umbo coincide with the intercostal sulci and costae of the exterior, simulating along the anterior margin of any growth stage a series of truly concentric folds through which

the thickness of the shell remains constant. In the postero-central region, however, the interior of the pedicle valve is considerably modified by the attachment areas of the muscles (Pl. 67, figs. 9, 14). On either side of the mid-line of the valve two large (length 12–15 mm., maximum width 5–6 mm.), flabellate diductor scars diverge away from the umbo; each is longitudinally ridged. Posteriorly the diductor scars meet, but at a distance of approximately 5 mm. from the hinge-line they become separated by an upraised platform 1.5–2 mm. high, 5–6 mm. long, and 2–2.25 mm. wide. This is the adductor platform and it bears two ovate adductor scars near its posterior end, each 1 mm. wide and 3 mm. long. At a distance of approximately 1 mm. from the umbo the posterior margin of the pedicle valve becomes internally thickened; on occasion the internal thickening forms a distinct ridge up to 0.5 mm. high. Laterally this thickening or ridge bends towards the anterior and passes into the sharp flexure which abruptly demarcates the visceral cavity from the ears.

The interior surface of the pedicle valve is roughened by the anteriorly projecting calcicular rods of the taleolae. The density of the taleolae (i.e. the number per unit length of the pedicle valve measured in thin section) ranges from 0–15 per mm. in various parts of the valve, with a mean density of 11 per mm. for the anterior region of the visceral disc and trail. Most of the taleolae are curved, forming a low angle with the plane of the shell surface at their termination within the shell substance, but projecting from the interior of the valve at an angle of approximately 50–70° to the valve surface.

#### EXTERNAL SURFACE OF BRACHIAL VALVE

The concave external surface of the brachial valve is costate and weakly rugate (Pl. 67, fig. 3). The costation is the exact reflection of that of the exterior surface of the pedicle valve, the costae of the latter being represented by the intercostal sulci of the brachial valve exterior. The postero-central portion of the valve is featureless except for a small protuberance situated on the hinge-line or the umbo (text-fig. 9). Up to six ill-defined rugae may occur, at least half the number being incomplete. The ears are demarcated from the rest of the shell by sharp folds which increase in amplitude towards the margin of the flanks and are complementary to the grooves demarcating the ears from the visceral disc of the pedicle valve. On two specimens several broken spines have been observed projecting at high angles to the anterior part of the visceral disc. The exterior surface of the brachial valve is otherwise smooth except for growth lamellae which are irregularly spaced but of the order of 7–9 per mm., as on the pedicle valve.

#### INTERNAL STRUCTURE OF BRACHIAL VALVE

Internally the bilateral symmetry of the brachial valve (Pl. 67, figs. 4, 7, 10) is reflected on either side of a slender median septum which extends 70–90% of the valve length from the posterior margin. The median septum has a mean length of  $8.4 \pm 0.5$  mm. (Table 1), and consists of two structural elements. The anterior 55% of the structure has a triangular blade-like form, 0.2–0.3 mm. wide, which arises from a position level with, or anterior to, the mid-point of the adductor scars. Towards the anterior the blade increases in height attaining a maximum elevation at, or within 0.5 mm. of, its anterior termination; the mean value for the maximum height of the median septum is  $1.33 \pm 0.28$  mm. (Table 1). The posterior section of the median septum is less well defined, comprising a low structure, semicircular in cross-section, with a maximum width of approximately

1 mm. and a maximum height of approximately 0.4 mm. Anteriorly it is contiguous with the blade-like portion of the septum; posteriorly it expands and fuses with the inflated ends of the marginal ridges to form a reinforced attachment with the cardinal process (Pl. 67, figs. 4, 10). In those specimens with a large cardinal process the posterior section of the median septum is weakly developed with an elevation of usually no more than 0.1 mm. The contour of the brachial valve is modified immediately anterior to the cardinal process by a dorsally concave and ventrally convex fold. The amplitude of this fold is slight with a maximum value of approximately 1.5 mm.; in shape it is elliptical with the long axis (3–6 mm.) orientated in a posterior to anterior direction. When the posterior section of the median septum is reduced in size the amplitude of the fold is generally large (1–1.5 mm.), the corrugation of the valve appearing, therefore, to compensate in part for the rigidity of a robust shaft. The value for the coefficient of correlation ( $r = 0.458$ ) of the length and height of the median septum is not significant, and similarly there is no simple relationship between the size of the median septum and the size of the visceral cavity.

#### TYPES OF CARDINAL PROCESS AND MUSCLE SCARS

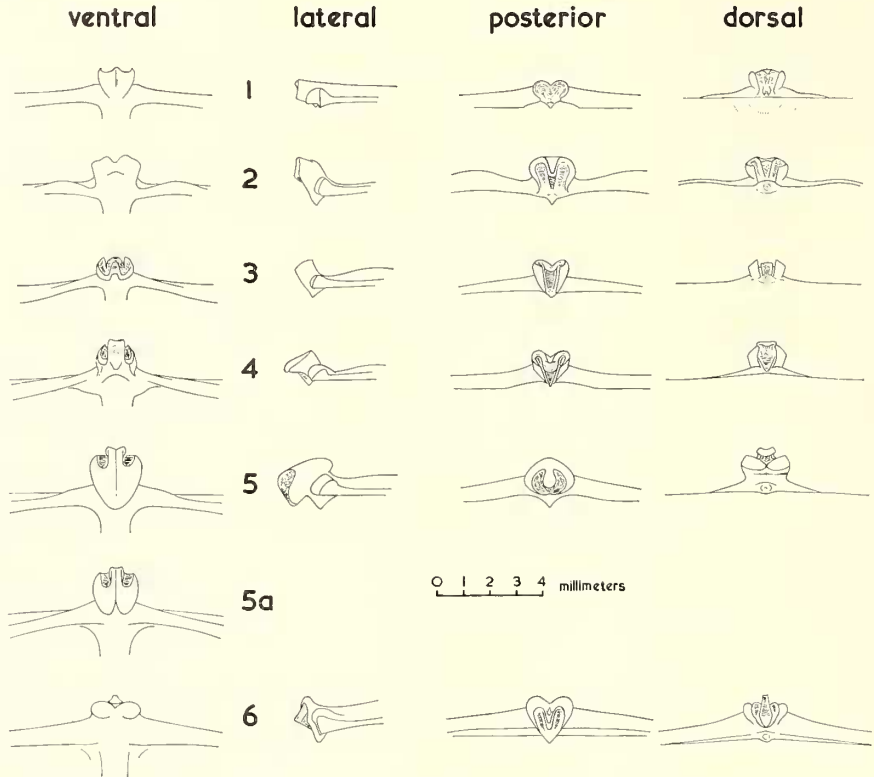
The cardinal process is a highly variable structure assuming a general costispiniferid form (Muir-Wood and Cooper 1960, pp. 28–29). It is trilobed, usually with a small median lobe, and is sessile; the overall dimensions are given in Table 1. Different types may be distinguished according to the degree of separation of the lateral lobes, and the inclination of the process with regard to the surface of the brachial valve (text-fig. 9; Pl. 67, figs. 4, 7, 10).

Type 1 (text-fig. 9–1; Pl. 67, fig. 4) is characterized by a horizontal posterior to anterior axis of the lateral lobes so that the process is in effect a lobed termination to the median septum. At the posterior extremity all three lobes are distinct, the small median lobe being little more than a V-shaped inflexion between the semiconical lateral lobes. The axis of the median lobe is disposed at  $50^\circ$  to the valve surface, and the anterior end continues into a distinct protuberance on the dorsal surface. The attachment area is directed postero-dorsally and the surface is roughened by the accentuation of growth lamellae. In ventral aspect the lateral lobes converge towards a mid-line before becoming fused anteriorly with the median septum. The cardinal process is buttressed by the swollen ends of the marginal ridges.

The cardinal process of type 2 (text-fig. 9–2) rises ventrally from the plane of the posterior part of the brachial valve at a steep angle ( $60^\circ$ ). When viewed from the posterior, two inflated lateral lobes are separated by a narrow median lobe which has a considerable extension in a postero-dorsal direction so that it makes an angle of only  $30^\circ$  with the brachial valve surface. The flexuous surface to which the diductor muscles were attached is roughened by irregular growth lamellae. Anterior to the median lobe the hinge-line bears a conspicuous protuberance which extends dorsally for approximately 0.3 mm. at right angles to the valve surface. In ventral aspect the lateral lobes converge and join the expanded end of the median septum.

The third type of cardinal process (text-fig. 9–3) has a similar upturned attitude in relation to the posterior part of the brachial valve to that of type 2. It differs from type 2, however, in the erect position of the median lobe and the anterior extension of the attachment surfaces of the lateral lobes, two features that enable the sinuous profile of the

complete attachment surface to be clearly seen in the ventral aspect of the valve. The attachment surface is almost normal to the plane of the valve and is made asperous by uneven growth lamellae. Dorsally the cardinal process tapers into a distinct protuberance which has a relief of 0.2–0.3 mm., at right angles to the exterior surface of the valve. The process is supported by the marginal ridges which rise ventrally and fuse with the lateral lobes.



TEXT-FIG. 9. Variation in the form of the cardinal process of *P. trearnensis*.

The strong median lobe of type 4 (text-fig. 9–4) distinguishes it from the other types of cardinal process. The general attitude of the process is similar to that of types 2 and 3 but the median lobe extends further postero-dorsally and is much incurved, forming a lip which overhangs the attachment surface. The ventral surface of the median lobe is concave and bears a small pit. The axis of the median lobe curves slightly but is approximately at an angle of 50° to the plane of the posterior part of the brachial valve. Dorsally the tip of the median lobe forms a small protuberance. The attachment surfaces of the lateral lobes are almost closed by the enlargement of the median lobe; the whole of the attachment surface is roughened by uneven growth lamellae. In ventral aspect the cardinal process is supported by a swelling of the marginal ridge–median septum inter-angle.

The cardinal process of type 5 (text-fig. 9–5; Pl. 67, fig. 7) is distinguished both by its size and attitude in relation to the brachial valve. The process is bulbous and its axis has

an antero-ventral to postero-dorsal incline, making an acute intersection with the brachial valve at  $40^\circ$ . The lateral lobes are much inflated and extended in an antero-ventral direction. In text-fig. 9-5 and Plac 67, fig. 7, the cardinal process has lateral lobes which are fused in a unified structure; the same type of cardinal process also occurs in which the lateral lobes are quite distinct anteriorly (text-fig. 9-5*a*). The median lobe is small and its dorsal extremity is posterior to the hinge-line and to a large protuberance 0.3-0.4 mm. in height which extends dorsally from the hinge-line at the mid-point of the valve. The involute attachment area is roughened in the usual way by growth lamellae. The cardinal process is supported by the thickened ends of the marginal ridges and the median septum.

The cardinal process of type 6 (text-fig. 9-6; Pl. 67, fig. 10) is similar to type 5 except that the incline of the process is increased so that the lateral lobes are directed dorsally, at right angles to the plane of the posterior part of the brachial valve. The median lobe has a conspicuous postero-dorsal extension, its axis being  $40^\circ$  to the surface of the valve. A protuberance extends dorsally, anterior to the median lobe. The attachment surface is roughened by growth lamellae and the process is supported by a swelling of the marginal ridges as they unite across the median septum.

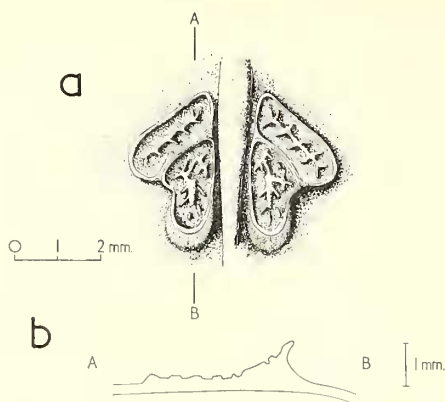
The distribution of the six types of cardinal process in a sample of 38 specimens is: type 1—7 specimens (18%), type 2—4 specimens (10.5%), type 3—6 specimens (16%), type 4—6 specimens (16%), type 5 and 5*a*—7 specimens (18%), type 7—8 specimens (21.5%).

The marginal ridges are asymmetrical elevations on the brachial valve which close the visceral cavity posteriorly and postero-laterally (Pl. 67, figs. 7, 10). From the cardinal process the ridges extend within  $7^\circ$  of the hinge-line a mean distance of  $6.1 \pm 0.5$  mm. (Table 1), before swinging anteriorly through an angle of  $110-145^\circ$  and continuing a mean distance of 4.5-6.5 mm. to their termination on the flanks. At the mid-point of the valve they join the median septum and frequently swell to support the cardinal process (text-fig. 9). The section of the marginal ridges which extends from a quarter to a half of the distance along the hinge-line from the median septum to the lateral extremity of the ears, represents the main articulating surface of the two valves. It is only in these two short lengths on either side of the cardinal process that the marginal ridges are sufficiently close to the posterior edge of the brachial valve for them to combine with the shell substance of the main part of the valve in producing a reinforced pivot against the strain of a crude leverage of the valves imposed by the contraction of the diductor muscles.

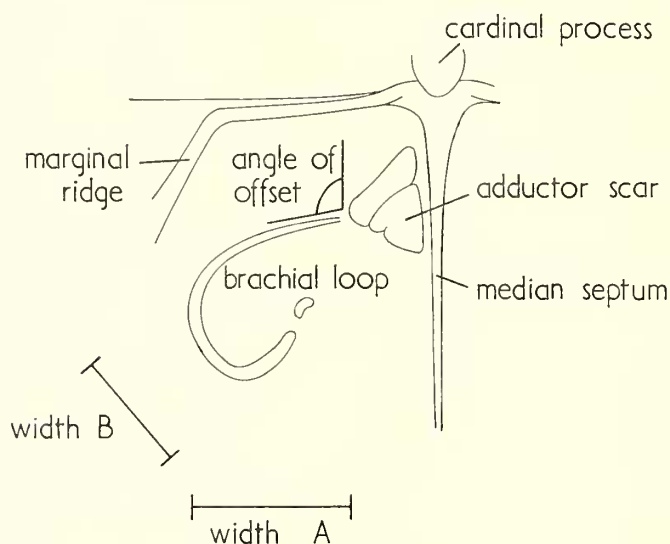
The adductor scars are two subtriangular elevated regions, the long sides of which are parallel to, and 0.1-0.3 mm. laterally separated from, the anterior blade of the median septum. The overall dimensions of the adductor scars and their location on the valve surface are given in Table 1. Each adductor scar has two main fields, each of which bears dendritic markings (text-fig. 10*a*). The anterior margin of the anterior field is steeply elevated above the valve surface (text-fig. 10*b*).

#### BRACHIAL RIDGES AND ENDOSPINES

The brachial ridges originate at the antero-lateral region of the adductor scars (Pl. 67, figs. 7, 10) and extend antero-laterally in a loop circumscribing a comparatively smooth, ovate area of the valve surface. The loop is incomplete at its anterior end (Pl. 67, fig. 7). The dimensions of the loop are given in Table 1; the positions of the measurements are shown in text-fig. 11.



TEXT-FIG. 10. (a) Reconstruction of adductor scars on either side of the median septum, each scar having two fields of attachment with dendritic relief. (b) Profile of adductor scar (section *AB* on (a)) showing steeply elevated anterior margin of the anterior field.



TEXT-FIG. 11. Diagram to show width *A*, width *B*, and angle of offset of the brachial loop (see Table 1).

It is estimated that 80–150 endospines extend anteriorly from the interior surface of the brachial valve. They are situated in a zone on the strongly convex anterior and antero-lateral slopes between the relatively flat postero-central disc and the trail. The majority are supracostal although others occur in sulci; they range in size up to 2 mm. and are inclined to the valve surface at approximately  $45^\circ$ . The taleolae of the brachial valve are variously distributed but attain a mean density of 11 per mm. at the anterior of the visceral disc and trail. As with the taleolae of the pedicle valve they are curved and anteriorly directed.

## APPENDIX OF TAXONOMIC DATA

TABLE 1

Linear measurements in millimetres, angular measurements in degrees

## Univariate Statistics of Selected Characters

<i>Character</i>	<i>N</i>	$\bar{x}$	<i>s</i>	<i>OR</i>	<i>V</i>	$\mu$ ( <i>P</i> = 0.05)	$\mu$ ( <i>P</i> = 0.01)
Hinge width of pedicle valve	45	17.3	2.49	13-22	14.38	16.6-18.0	16.3-18.3
Curved (or surface) length of pedicle valve	19	32.9	5.02	25-41	15.13	30.5-35.4	29.6-36.3
Straight length	19	13.6	1.42	11.4-17.2	10.43	12.9-14.3	12.7-14.5
Thickness (or height) of visceral cavity inclusive of shell	29	5.4	1.82	4.0-9.5	24.70	5.0-5.9	4.8-6.1
Width of sulcus	18	5.9	1.39	3-8	23.73	5.2-6.5	4.9-6.8
Depth of sulcus	18	0.87	0.356	0.5-1.5	40.69	0.70-1.05	0.63-1.12
Width of flat zone on venter of non-sulcate forms	26	4.5	1.98	1-8	45.47	3.5-5.1	3.3-5.4
Umbonal angle	32	99.5	9.81	85-135	9.86	95.9-103.0	94.7-104.1
Extension of umbo posterior to hinge	32	0.75	0.245	0.3-1.3	32.65	0.66-0.83	0.63-0.87
Ear width	27	7.32	1.12	5-10	15.20	6.47-8.17	6.17-8.47
Ear length	27	3.03	0.606	2-4	19.99	2.79-3.27	2.70-3.36
Ear height	27	0.85	0.351	0.2-1.7	41.32	0.71-0.99	0.66-1.04
Number of costae	34	26.0	4.42	18-39	16.99	25-27	24-28
Number of rugae	36	7.0	2.14	3-13	30.51	6-8	6-8
Length of median septum	22	8.4	0.91	7.0-10.5	9.91	8.02-8.83	7.87-8.97
Height of median septum at anterior end	16	1.33	0.38	0.7-1.9	28.74	1.13-1.53	1.05-1.61
Length of cardinal process	33	0.94	0.34	0.6-1.9	36.5	0.86-1.02	0.83-1.05
Width of cardinal process	33	1.17	0.26	0.6-1.7	22.4	1.08-1.27	1.05-1.30
Length of marginal ridge along posterior margin	11	6.1	0.54	5.3-7.0	8.89	5.74-6.46	5.56-6.62
Height of marginal ridge along posterior margin	28	0.25	0.064	0.2-0.4	25.53	0.22-0.27	0.21-0.28
Width of marginal ridge along posterior margin	28	0.32	0.121	0.2-0.6	37.12	0.28-0.37	0.26-0.39
Length of adductor scar	19	2.43	0.40	1.7-3.3	16.56	2.23-2.62	2.16-2.69
Width of adductor scar	20	1.61	0.29	1.3-2.5	17.91	1.48-1.75	1.43-1.80
Distance of posterior end of adductor scar from hinge-line	18	1.88	0.28	1.3-2.3	15.15	1.75-2.03	1.69-2.08
Distance of adductor scar from median septum	17	0.17	0.069	0.1-0.3	40.21	0.13-0.21	0.12-0.22
Width <i>A</i> of brachial loop	5	4.28	0.415	4.0-5.0	9.69	3.76-4.79	3.43-5.13
Width <i>B</i> of brachial loop	5	3.40	0.447	2.8-4.0	13.15	2.16-4.64	1.34-5.46
Angle of offset of brachial ridges	5	104	8	95-110	7.9	94-114	87-121
Width of brachial ridge	5	0.27	0.097	0.15-0.40	36.10	0.15-0.39	0.07-0.47
Distance of posterior end of brachial ridge from hinge-line	5	3.50	0.436	3.0-4.0	12.45	2.96-4.04	2.60-4.38

TABLE 2

Measurements to compare the relative increase in the length of the Brachial Valve and the thickness of the Visceral Cavity for unit increases in the length of the Pedicle Valve

<i>Number of increments</i>	<i>Curved length of p.v.</i>	<i>Increment to curved length of b.v.</i>	<i>Curved length of b.v.</i>	<i>Increment to thickness of visceral cavity</i>	<i>Thickness of visceral cavity</i>
1	2.5	2.08	2.08	—	—
2	5.0	1.75	3.83	—	0.83
3	7.5	1.58	5.41	0.42	1.25
4	10.0	1.54	6.95	0.42	1.67
5	12.5	1.33	8.28	0.42	2.09
6	15.0	0.92	9.20	0.42	2.51
7	17.5	0.75	9.95	0.42	2.93
8	20.0	0.34	10.29	0.59	3.43
9	22.5	0.29	10.58	0.66	4.09
10	25.0	0.67	11.25	0.75	4.84
11	27.5	0.91	12.16	0.83	5.67
12	30.0	1.92	14.08	0.66	6.33
13	32.5	2.42	16.50	0.50	6.83
14	35.0	2.50	19.00		
15	37.5	2.50	21.50		

TABLE 3

Measurements to compare the relative increase in the thickness of the Visceral Cavity for unit increase in the length of the Brachial Valve

<i>Number of increments</i>	<i>Curved length of b.v.</i>	<i>Increment to thickness of visceral cavity</i>	<i>Thickness of visceral cavity</i>
1	0.8		
2	1.7		
3	2.5		0.58
4	3.3	0.08	0.66
5	4.2	0.21	0.87
6	5.0	0.21	1.08
7	5.8	0.21	1.29
8	6.7	0.21	1.50
9	7.5	0.21	1.71
10	8.3	0.21	1.92
11	9.2	0.21	2.13
12	10.0	0.25	2.38
13	10.8	0.29	2.67
14	11.7	0.41	3.08
15	12.5	0.92	4.00
16	13.3	1.17	5.17
17	14.2	0.83	6.00
18	15.0	0.17	6.17

TABLE 4  
Bivariate statistics of Selected pairs of Characters

<i>Characters</i>	<i>N</i>	<i>Coefficient of correlation</i>	<i>Coefficient of relative dispersion about reduced major axis</i>	<i>Level of significance</i>
Hinge width × curved length	19	0.681	11.58	0.01
Hinge width × straight length	19	0.536	10.83	0.05
Sulcation: width × depth	18	0.467	25.01	not significant
Thickness of visceral cavity × sulcation	10	-0.141	—	not significant
Umbonal angle × extension of umbo posterior to hinge	32	0.351	11.23	0.05
Extension of umbo posterior to hinge × thickness of visceral cavity	23	0.500	26.01	0.05
Umbonal angle × hinge width	29	-0.285	—	not significant
Hinge width × ear width	27	0.729	11.58	0.01
Ear width × ear length	27	0.428	17.97	0.05
Ear width × ear height	27	0.095	29.67	not significant
Ear length × ear height	27	0.181	51.46	not significant

TABLE 5

Measurements showing the changing proportions of the Ventral Sulcus

<i>Position on valve surface</i>	<i>Distance from umbo</i>	<i>Width of sulcus</i>	<i>Depth of sulcus</i>
Posterior of visceral disc	0-0.85	nonsulcate	nonsulcate
Mid-region of visceral disc	0.85-1.05	3.0	0.25
	1.05-1.25	4.0	0.50
	1.25-1.75	5.0	0.75
Anterior of visceral disc	1.75-2.25	5.0	1.00
Trail	2.25-2.60	5.0	0.75
	2.60-3.35	5.0	0.50

TABLE 6

Variation in Costation of the Pedicle Valve

A—REGULAR COSTATION  (costae approximately equal in width)	<i>Width</i>		<i>Nature of cross-section</i>
	Fine < 1.2 mm.	Coarse > 1.2 mm.	
	Group 1	Group 4	Rounded
		Group 6	Scalloped
B—IRREGULAR COSTATION	<i>Range of mean widths</i>		<i>Nature of cross-section</i>
	No. of Fine > Coarse Mean width < 1.0 mm.	No. of Coarse > Fine Mean width > 1.0 mm.	
	Group 2	Group 3	Rounded
		Group 5	Rounded & scalloped